Inorg. Chem. **2005**, *44*, 5278–5285

Syntheses, Crystal Structures, and Luminescent Properties of Three Novel Zinc Coordination Polymers with Tetrazolyl Ligands

Xi-Sen Wang,[†] Yun-Zhi Tang,[†] Xue-Feng Huang,[†] Zhi-Rong Qu,[†] Chi-Ming Che,[‡] Philip Wai Hong Chan,[‡] and Ren-Gen Xiong*[,†]

Coordination Chemistry Institute, The State Key Laboratory of Coordination Chemistry, Nanjing University, 210093 Nanjing, P. R. China, and Department of Chemistry, The University of Hong Kong, Pokfulam Road, Hong Kong, P. R. China

Received March 7, 2005

The syntheses and luminescent properties of three novel zinc coordination polymers containing tetrazolyl ligands are described. In situ [2+3] cycloaddition reactions of acetonitrile or *p*-tolylnitrile with sodium azide in the presence of $Zn(ClO_4)_2$ as a Lewis acid (Demko–Sharpless tetrazole synthesis method) under hydrothermal (solvothermal) reaction conditions gave $[Zn(CH_3CN_4)_2]_3(H_2O)$ (**1**) and $[Zn(4\text{-MPTZ})_2]$ (**3**) [4-MPTZ = 5-(4-methylphenyl)tetrazole], respectively. On the other hand, $[Zn(HCN_4)_2]$ (**2**) was obtained by directly reacting tetrazole with $Zn(OAc)_2$ under hydrothermal reaction conditions. The structure of **1** shows a super-diamond-like topological network with a diamond subunit as a connecting node. For **2**, a diamond-like topological network is also found, but it is 2-fold interpenetrated. The structure of **3** reveals a 2D layered network with a hexagonal net, with the adjacent layers in the network stacked in an ABAB sequence. Photoluminescence studies revealed coordination polymers **1**, **2**, and **3** exhibit strong blue fluorescent emissions at λ_{max} = 396, 418, and 397 nm, respectively, in the solid state at room temperature.

Introduction

The tetrazole functional group has found a wide range of applications in coordination chemistry as ligands, in medicinal chemistry as a metabolically stable surrogate for a carboxylic acid group, and in materials science as high-density energy materials.[1] Of interest to supramolecular chemists is the coordination ability of the tetrazolyl ligand through the four nitrogen electron-donating atoms that allows it to serve as either a multidentate or a bridging building block in supramolecular assemblies. Indeed, the tetrazole ligand has been shown to be able to participate in at least seven distinct types of coordination modes with metal ions in the construction of novel metal-organic frameworks. As shown in Scheme 1, the nitrogen-containing heterocycle can either coordinate in a μ_1-tetrazolyl (Mode I); μ_2-tetrazolyl

Scheme 1

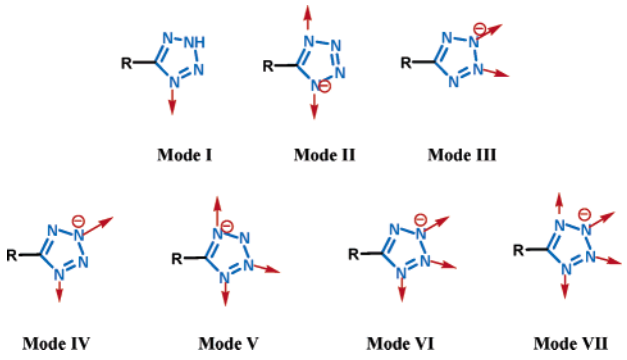

mode, which in itself has three different modes of coordination (Modes II−IV); adopt two different μ_3-tetrazolyl modes (Modes V−VI); or act in a μ_4-tetrazolyl mode (Mode VII). In this context, it is not surprising to find in the literature the development of numerous synthetic routes to this ubiquitously useful functional group.[1−4] Despite these ad-

* Author to whom correspondence should be addressed. E-mail: Xiongrg@netra.nju.edu.cn.
[†] Nanjing University.
[‡] The University of Hong Kong.

(1) (a) Wittenberger, S. J. *Org. Prep. Proced. Int.* **1994**, *26*, 499. (b) Dunica, J. V.; Pierce, M. E.; Santella, J. B., III. *J. Org. Chem.* **1991**, *56*, 2395. (c) Wittenberger, S. J.; Donner, B. G. *J. Org. Chem.* **1993**, *58*, 4139. (d) Curran, D. P.; Hadida, S.; Kim, S.-Y. *Tetrahedron* **1999**, *55*, 8997.

(2) (a) Wiberg, V. E.; Michaud, H. *Z. Naturforsch., B: Chem. Sci.* **1954**, *9*, 497. (b) Grzonka, Z.; Staszak, M. A.; Liberek, B. *Rocz. Chem.* **1971**, *45*, 967. (c) Huff, B. E.; Staszak, M. A. *Tetrahedron Lett.* **1993**, *34*, 8011. (d) Kumar, A.; Narayanan, R.; Shechter, H. *J. Org. Chem.* **1996**, *61*, 4462.

10.1021/ic050354x CCC: $30.25
Published on Web 06/30/2005

vances, methodologies that do not need the use of expensive and toxic metal-organic azide complexes such as tin or silicon organic azides, the application of highly moisture-sensitive reaction conditions, or the use of hydrazoic acid, which is extremely toxic, volatile, and explosive, remain sparse. A recent notable achievement by Sharpless and co-workers showed that a safe, convenient, and environmentally friendly synthetic route to 5-substituted 1*H*-tetrazoles can be accomplished with water as a solvent and zinc salts as a catalyst.[5] However, little is known about the exact role of the zinc catalyst, and the mechanistic pathway(s) in this new synthesis of tetrazoles remains unclear.

Recently, works in our laboratory have focused on in situ construction and crystallographic characterization of functionally novel supramolecular motifs under hydrothermal conditions[6] and the application of such studies to investigating the possible intermediates formed during the Demko−Sharpless [2+3] cycloaddition reaction.[4] The structural characterization of such intermediates may provide important clues to the mechanistic role of the metal species and provide an invaluable insight to the reaction mechanism that may, in turn, allow synthetic chemists to further optimize reaction conditions. As part of our continuing interest to understanding the mechanism of the Demko−Sharpless tetrazole reaction and the synthetic usefulness of hydrothermal reactions, we describe, herein, the synthesis of three novel zinc coordination polymers containing tetrazolyl ligands. The isolation and structural characterization of the three zinc coordination polymers by X-ray crystallography and a study of their luminescence properties are also presented.

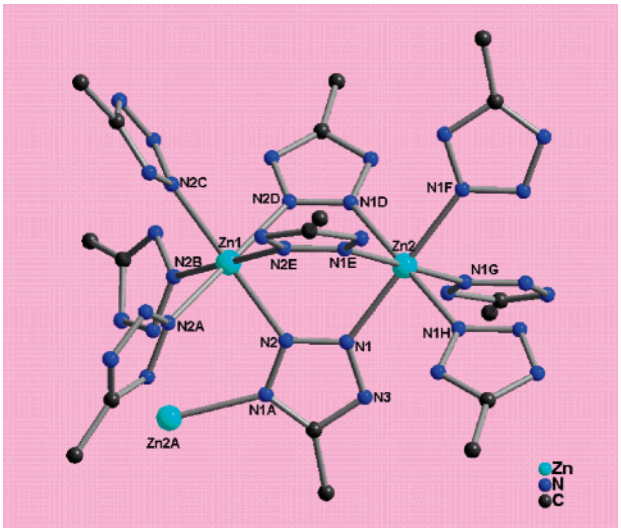

Figure 1. Asymmetric unit representation of **1**.

Scheme 2

$$CH_3CN + Zn(ClO_4)_2 + NaN_3 \xrightarrow[125\ ^{o}C]{H_2O/C_2H_5OH} \left[\left(H_3C-\text{tetrazolyl}\right)_6 Zn_3\right](H_2O) \quad (1)$$

Results and Discussion

Preparation and Structures of 1−3. The reaction of $Zn(ClO_4)_2$ and MeCN under hydrothermal conditions at a temperature of 125 °C gave the coordination polymer $[Zn(CH_3CN_4)_2](H_2O)_4$ (**1**) as colorless prismatic crystals in ca. 60% yield (Scheme 2). Product formation of **1** was based on elemental analyses and IR spectroscopic measurements revealing the absence of a cyano peak in the 2200 cm^{-1} region of the spectrum, which is present in the IR spectrum of the starting material. This suggests the in situ reaction of this functionality with sodium azide by the Sharpless tetrazole synthesis protocol to give the tetrazole group, as evidenced by the presence of a new stretching frequency at ca. 1400 cm^{-1}. A broad peak at 3400∼3500 cm^{-1} is tentatively attributed to the coordination of four water molecules to the metal center in **1** as well as the possible presence of uncoordinated water molecules.

The IR spectrum and elemental analyses of **1** are consistent with structural determination of the polymeric complex by X-ray crystallography, which shows one unique ligand and one unique zinc center persisting in **1**. As shown in Figure 1, it is clear to see that the newly formed 5-methyltetrazole ligand acts as a tridentate bridging ligand that is Mode VI-coordinated to the Zn^{2+} ions. Each ligand is bound to three Zn centers, and each Zn atom is bound to six ligands. The local coordination environment around the Zn(1) center forms a perfect octahedron, as evidenced by their bond angles (90 and 180°) shown in Table 1. The Zn−N distances in **1** range

(3) (a) Carlucci, L.; Ciani, G.; Proserpio, D. M. *Angew. Chem., Int. Ed.* **1999**, *38*, 3488. (b) Singh, H.; Chawla, A. S.; Kapoor, V. K.; Paul, D.; Malhotra, R. K. *Prog. Med. Chem.* **1980**, *17*, 151. (c) Ostrovskii, V. A.; Pevzner, M. S.; Kofmna, T. P.; Shcherbinin, M. B.; Tselinskii, I. V. *Targets Heterocycl. Syst.* **1999**, *3*, 467. (d) Janiak, C. *J. Chem. Soc., Chem. Commun.* **1994**, 545. (e) Janiak, C.; Scharmann, T. G.; Gunter, W.; F. Girgsdies, F.; Hemling, H.; Hinrichs, W.; Lentz, D. *Chem.−Eur. J.* **1995**, *1*, 637. (f) Bhandari, S.; Mahon, M. F.; McGinley, J. G.; Molloy, K. C.; Roper, C. E. E. *J. Chem. Soc., Dalton Trans.* **1998**, 3425. (g) Hill, M.; Mahon, M. F.; Molloy, K. C. *J. Chem. Soc., Dalton Trans.* **1996**, 1857. (h) Bhandari, S.; Mahon, M. F.; Molloy, K. C.; Palmer, J. S.; Sayers, S. F. *J. Chem. Soc., Dalton Trans.* **2000**, 1053. (i) Zhou, X.-G.; Huang, Z.-A.; Cai, R.-F.; Zhang, L.-X.; Hou, X.-F.; Feng, X.-J.; Huang, X.-Y. *J. Organomet. Chem.* **1998**, *563*, 101.

(4) (a) Xiong, R.-G.; Xue, X.; Zhao, H.; You, X.-Z.; Abrahams, B. F.; Xue, Z. *Angew. Chem., Int. Ed.* **2002**, *41*, 3800. (b) Xue, X.; Wang, X.-S.; Wang, L.-Z.; Xiong, R.-G.; Abrahams, B. F.; You, X.-Z.; Xue, Z.; Che, C.-M. *Inorg. Chem.* **2002**, *41*, 6544. (c) Xue, X.; Abrahams, B. F.; Xiong, R.-G.; You, X.-Z. *Aust. J. Chem.* **2002**, *55*, 495. (d) Wang, L.-Z.; Wang, X.-S.; Li, Y.-H.; Bai, Z.-P.; Xiong, R.-G.; Xiong, M.; Li, G.-W. *Chin. J. Inorg. Chem.* **2002**, *18*, 1191. (e) Wang, L.-Z.; Qu, Z.-R.; Zhao, H.; Wang, X.-S.; Xiong, R.-G.; Xue, Z. *Inorg. Chem.* **2003**, *42*, 3969. (f) Qu, Z.-R.; Zhao, H.; Wang, X.-S.; Li, Y.-H.; Song, Y.-M.; Liu, Y.-J.; Ye, Q.; Xiong, R.-G.; Abrahams, B. F.; Xue, Z.; You, X.-Z. *Inorg. Chem.* **2003**, *42*, 7710. (g) Zhao, H.; Ye, Q.; Wu, Q.; Song, Y.-M.; Liu, Y.-J.; Xiong, R.-G. *Z. Anorg. Allg. Chem.* **2004**, *630*, 1367. (h) Ye, Q.; Li, Y.-H.; Song, Y.-M.; Huang, X.-F.; Xiong, R.-G.; Xue, Z. *Inorg. Chem.* **2005**, *44*, 3618. (i) Huang, X.-F.; Song, Y.-M.; Wu, Q.; Ye, Q.; Chen, X.-B.; Xiong, R.-G.; You, X.-Z. *Inorg. Chem. Commun.* **2005**, *8*, 58. (j) Wang, X.-S.; Huang, X.-F.; Xiong, R.-G.; Chin, J. *Inorg. Chem.* **2005**, *21*, 1020. (k) Wang, X.-S.; Tang, Y.-Z.; Xiong, R.-G.; Chin, J. *Inorg. Chem.* **2005**, *21*, 1025. (l) Wang, X.-S.; Song, Y.-M.; Xiong, R.-G.; Chin, J. *Inorg. Chem.* **2005**, *21*, 1030.

(5) (a) Demko, Z. P.; Sharpless, K. B. *J. Org. Chem.* **2001**, *66*, 7945. (b) Demko, Z. P.; Sharpless, K. B. *Org. Lett.* **2001**, *3*, 4091. (c) Himo, F.; Demko, Z. P.; Noodleman, L.; Sharpless, K. B. *J. Am. Chem. Soc.* **2002**, *124*, 12210. (d) Demko, Z. P.; Sharpless, K. B. *Org. Lett.* **2002**, *4*, 2525. (e) Demko, Z. P.; Sharpless, K. B. *Angew. Chem., Int. Ed.* **2002**, *41*, 2110. (f) Demko, Z. P.; Sharpless, K. B. *Angew. Chem., Int. Ed.* **2002**, *41*, 2113. (g) Himo, F.; Demko, Z. P.; Noodleman, L.; Sharpless, K. B. *J. Am. Chem. Soc.* **2003**, *125*, 9983.

(6) (a) Xiong, R.-G.; Zhang, J.; Chen, Z.-F.; You, X.-Z.; Che, C.-M.; Fun, H.-K. *J. Chem. Soc., Dalton* Trans. **2001**, 780. (b) Xiong, R.-G.; You, X.-Z.; Abrahams, B. F.; Xue, Z.; Che, C.-M. *Angew. Chem., Int. Ed.* **2001**, *40*, 4422.

Table 1. Crystal Data Collection and Structure Refinement

	1	2	3
empirical formula	$C_{12}H_{20}N_{24}OZn_3$	$C_2H_2N_8Zn$	$C_{16}H_{14}N_8Zn$
fw	712.63	203.49	383.72
cryst syst	cubic	orthorhombic	orthorhombic
space group	$Fd\bar{3}m$	*Pbca*	*Pbcn*
cryst dimensions	0.2 × 0.1 × 0.1	0.2 × 0.15 × 0.1	0.2 × 0.1 × 0.08
a (Å)	17.6019(12)	9.885(2)	10.1580(11)
b (Å)	17.6019(12)	9.536(2)	13.9511(15)
c (Å)	17.6019(12)	13.724(3)	25.643(3)
α (deg)	90	90	90
β (deg)	90	90	90
γ (deg)	90	90	90
V (Å^3)	5453.5(6)	1293.8(5)	3634.0(3)
Z	8	8	8
F(000)	2864	800	1568
ρ_{calcd} (g cm^{-3})	1.736	2.089	1.403
μ (mm^{-1})	2.675	3.735	1.367
R1 [$I > 2\sigma(I)$]	0.0425	0.0274	0.0534
wR2 [$I > 2\sigma(I)$]	0.1110	0.0596	0.0689
R1 (all data)	0.0692	0.0400	0.2637
wR2 (all data)	0.1282	0.0630	0.1072
GOF	0.921	0.918	0.692

from 2.163 to 2.166 Å and are in good agreement with literature values for Zn−tetrazole complexes, whereas the C−C and C−N distances are unexceptional.

The role of the 5-methyltetrazole ligand, in which the methyl groups show significant disorder, is that of a tridentate bridging spacer that connects three Zn centers together results in the formation of a three-dimensional coordination network as shown in (Figure 1). In this network, the methyltetrazole ligands form bridges to four equivalent Zn(2) centers that lie at the vertexes of a perfect tetrahedron, as shown in Figure 2. Tetrahedral units that contain a central Zn(1) center, six methyltetrazole ligands (one along each edge of the tetrahedron), and Zn(2) at the vertexes of the tetrahedron link together to form a diamond-like network. The Zn(2) center at each vertex is shared between two linked tetrahedral units. This subunit can be best described as an adamantine-type unit with the tetrahedral nodes represented by a tetrahedron formed from an octahedral arrangement of ligands around Zn1 with Zn2 lying at the vertexes of a perfect tetrahedron (Figure 3). The presence of tetrahedral and octahedral Zn2 centers results in the connected tetrahedrons. The Zn2−ligand separation is 3.294 Å within the diamondoid network. The Zn2−ligand−Zn2 and ligand−Zn2−ligand bond angles within the diamondoid network are 141.71° and 89.54°, respectively, and deviate significantly from the 109.47° expected for an idealized diamond network. The subunit is connected to four adjacent subunits through the zinc atoms and expands to give a 3D coordination network (Figure 4). Note that there are many different ways of linking four connected nodes together to give a variety of 4-connecting nets, and a diamond net is often the result. However, the only way of guaranteeing the diamond net is to ensure that the connections between tetrahedral nodes are all perfectly staggered (i.e., rotated 60° from the eclipsed conformation). By having an octahedral Zn center (lying on the −3m site) as the link between tetrahedral nodes, the staggered conformation is ensured, and a diamond network is the inevitable consequence. In this work, the network of **1** has the topology of the diamond net with a diamond subunit as the connecting

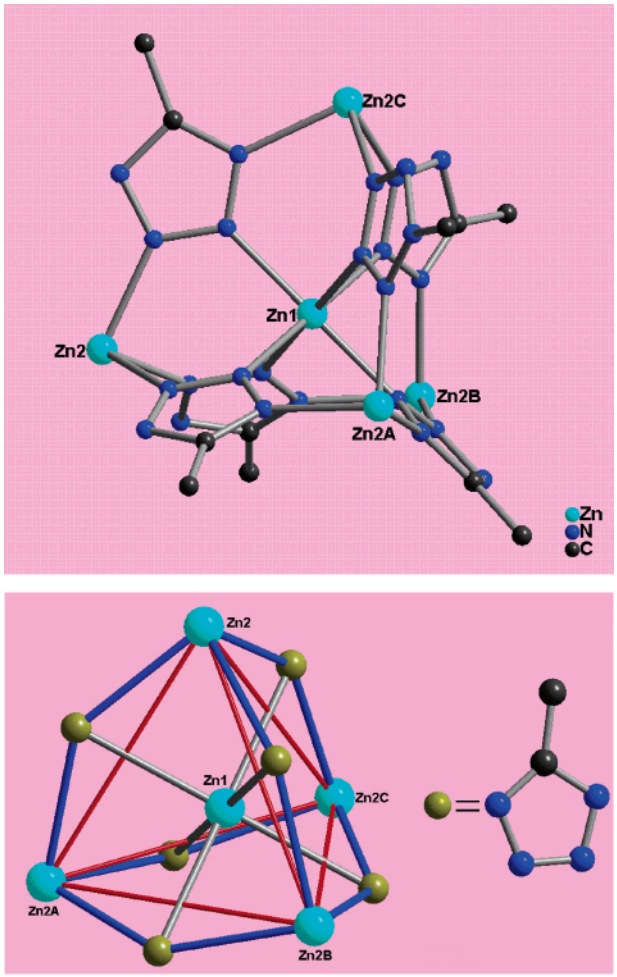

Figure 2. (a) Perspective view of the subunit in **1**. (b) Zn(1) lying in a tetrahedron center composed of four corners Zn2A, Zn2B, Zn2C, and Zn2D.

node (Figure 3) that can be called a super-diamond-like net. The Zn1−Zn1 separation is 7.622 Å within the diamondoid network. By omitting the subunit groups, the Zn1−Zn1−Zn1 angle in **1** (109.5°) is found to be very close to the expected value for an idealized diamond network (109.47°). To our knowledge, **1** is the first example of such a diamond-like network with a diamond subunit as the connecting node.[7]

Reaction of $Zn(OAc)_2$ with tetrazole under 2-butanolothermal conditions at 140 °C gave $[Zn(HCN_4)_2]$ (**2**) as colorless prismatic crystals in ca. 65% yield (Scheme 3). The IR spectrum of **2** shows peaks at 1346, 1367, and 1474 cm^{-1} assignable to the tetrazole group. As shown in Figure 5, the structure of **2** reveals the ligand is essentially planar and bound to only two Zn centers through two tetrazolyl N atoms with the coordination Mode II. Each Zn atom is coordinated

(7) For reviews on diamondoid-like networks: (a) Batten, S. R.; Robson, R. *Angew. Chem., Int. Ed.* **1998**, *37*, 1460. (b) Zaworotko, M. J. *Chem. Soc. Rev.* **1994**, *23*, 283. (c) Janiak, C. *Angew. Chem., Int. Ed. Engl.* **1997**, *36*, 1431. (d) Yaghi, O. M.; Li, H.; Davis, C.; Richardson, D.; Groy, T. L. *Acc. Chem. Res.* **1998**, *31*, 474. (e) Evans, O. R.; Lin, W.-B. *Acc. Chem. Res.* **2002**, *35*, 511. (f) Blake, A. J.; Champness, N. R.; Cooke, P. A.; Nicolson, J. E. B.; Wilson, C. *J. Chem. Soc., Dalton Trans.* **2000**, 3811. (g) Carlucci, L.; Ciani, G.; Proserpio, D. M.; Rizzato, S. *Chem.—Eur. J.* **2002**, *8*. 1520. (h) Hirsch, K. A.; Wilson, S. R.; Moore, J. S. *Chem.—Eur. J.* **1997**, *3*, 765. (i) Cheng, J.-K.; Chen, Y.-B.; Wu, L.; Zhang, J.; Wen, Y.-H.; Li, Z.-J.; Yao, Y.-G. *Inorg. Chem.* **2005**, *44*, 3386.

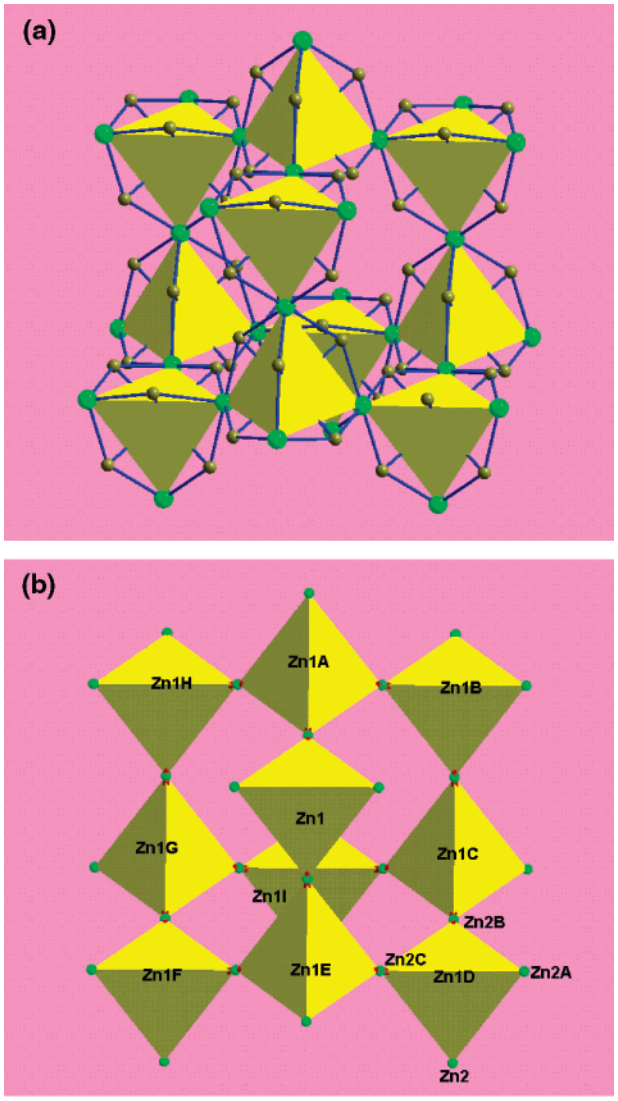

Figure 3. (a) Diamond net using corner-sharing tetrahedra in army-yellow represents a ligand. (b) Cristabolite-like diamond net using the corner-sharing tetrahedral representation in **1** in which Zn atoms represent the tetrahedral central atoms of the subunit.

by four such ligands to give rise to a distorted tetrahedral environment. The Zn−N distances range from 1.971 to 1.987 Å, which are slightly shorter than those found in **1**, and could probably be due to the lower coordination number around the Zn center and the absence of a methyl group in the tetrazole ring.

From a topological perspective view, each Zn center may be considered as a four-connecting node, which links to equivalent four-connecting centers through bridging tetrazole ligands. Since each of these ligands is only two-connecting, they are only considered as connections and not nodes. Consequently, this results in the formation of a 3D polymeric network with a diamondoid structure, as shown in Figure 6. The Zn−Zn separations are 5.989(1) and 6.016(1) Å within the diamond-like network. By removing the tetrazole groups in a similar manner as that for **1**, the Zn−Zn−Zn angles in **2** are revealed to range from 96.2° to 111.22° and deviate significantly from the expected 109.47° value for an idealized diamond network. This suggests compound **2**, thus, adopts a highly distorted diamond-like structure. As evidenced in

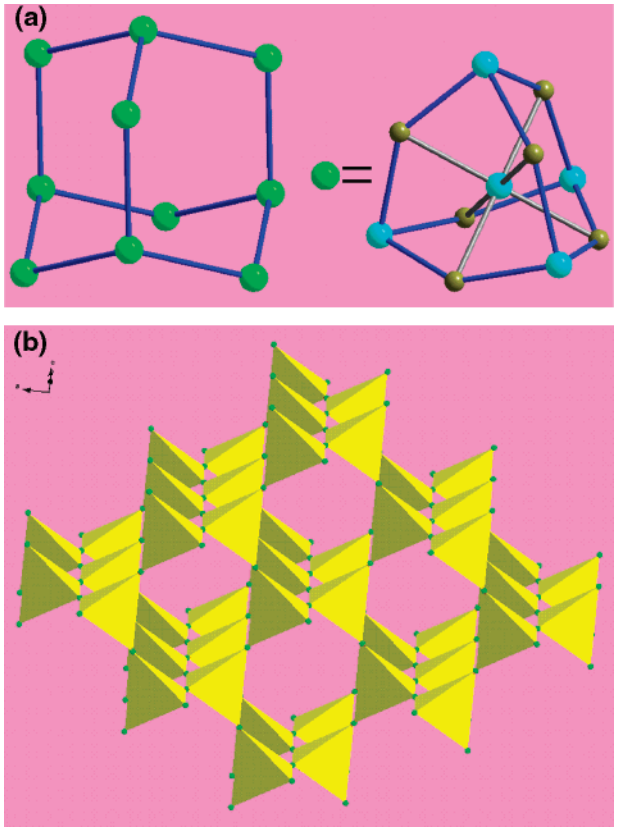

Figure 4. (a) Diamond-like net representation of **1** with a supertetrahedron as the connecting node. (b) Three-dimensional diamond-like network representation in which each supertetrahedron is highlighted in yellow and composed of a cristabolite-like 3D network.

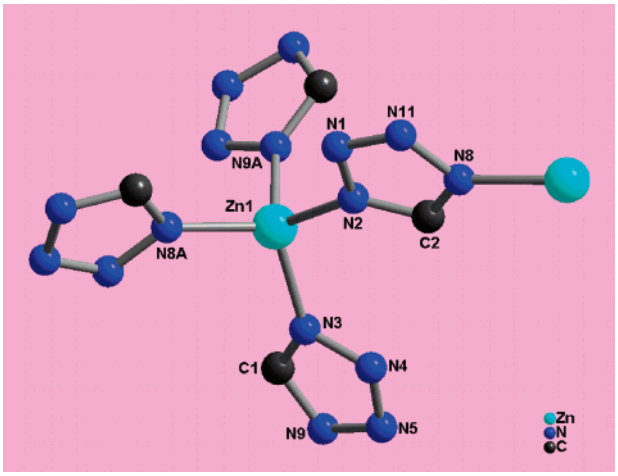

Figure 5. Asymmetric unit representation of **2**.

Scheme 3

Figure 6, a large cavity exists within a single diamond-like network. However, compound **2** avoids a potentially large open space by forming a 2-fold interpenetrated diamond-like structure (Figure 7).[7]

Under solvothermal conditions, reaction of $Zn(NO_3)_2$ with 4-methylbenzonitrile at 125 °C afforded $[Zn(4\text{-}MPTZ)_2]$ (**3**) as colorless prismatic crystals in ca. 75% yield (Scheme 4).

Scheme 4

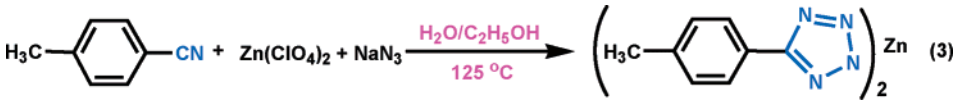

Structural elucidation of **3** was based on elemental analyses and an IR spectroscopic analysis showing the absence of a cyano peak in the 2100 cm^{-1} region, which is present in the starting material, and the appearance of a stretching frequency at ca. 1400 cm^{-1}. This shift in the peaks in the IR spectrum from 2100 to 1400 cm^{-1} would support that the proposed Demko−Sharpless [2+3] cycloaddition reaction between the nitrile group and sodium azide to give the tetrazole functionality had occurred.

The polymeric structure of **3** was determined by an X-ray single-crystal structure determination. Each asymmetric unit of **3** contains two Zn atoms and six tetrazolyl ligands. The local coordination geometry around the Zn center can be best described as a distorted tetrahedron with four N atoms from different tetrazolyl ligands with Zn−N bond distances ranging from 1.972 to 2.014 Å that are comparable to those found in **2** but slightly shorter than those found in **1** (Figure 8). The C−C, C−N, and N−N distances in **3** are also comparable to literature values. As shown in Figure 8, the 4-MPTZ ligands in **3** act as bidentate bridging ligands that are connected to Zn^{2+} ions in the Mode II and Mode III coordination modes. Each Zn center is linked to three other Zn centers through the bridging ligands. This leads to the formation of a 2D network containing a hexagonal net with a dimer unit as the connecting node, as shown in Figure 9. The adjacent layers in the network are stacked in an ABAB sequence, as depicted in Figure 10. However, in contrast to the local coordination environment around Zn centers in **1**, the local coordination geometry around Zn centers in **3** is tetrahedral rather than octahedral. One possible reason for this could be due to greater steric interactions between the *p*-tolyltetrazole groups in **3** compared to those of the methyltetrazole groups in **1**. In the case of **2**, on the other hand, the reason for adopting a tetrahedral local coordination

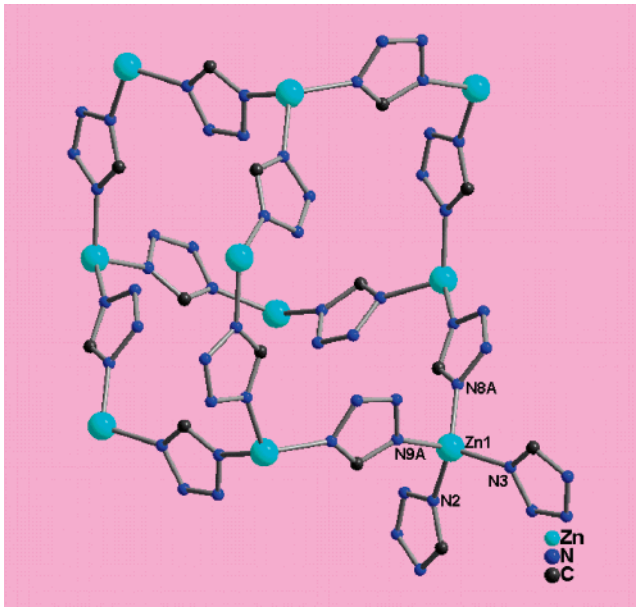

Figure 6. Diamondoid structure of **2**.

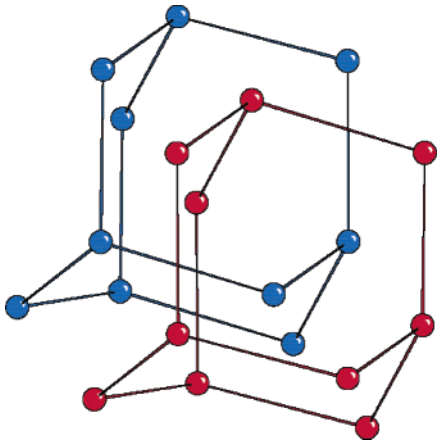

Figure 7. Diagram illustrating the triplicate interpenetration diamondoid structure in **2**. The long line represents tetrazole.

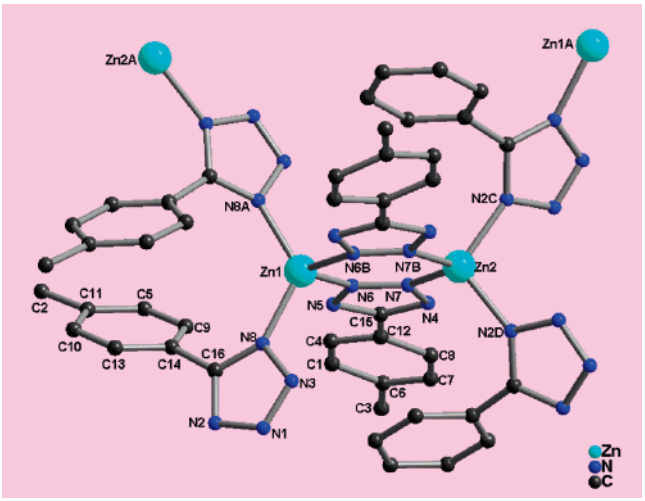

Figure 8. Asymmetric unit representation of **3**.

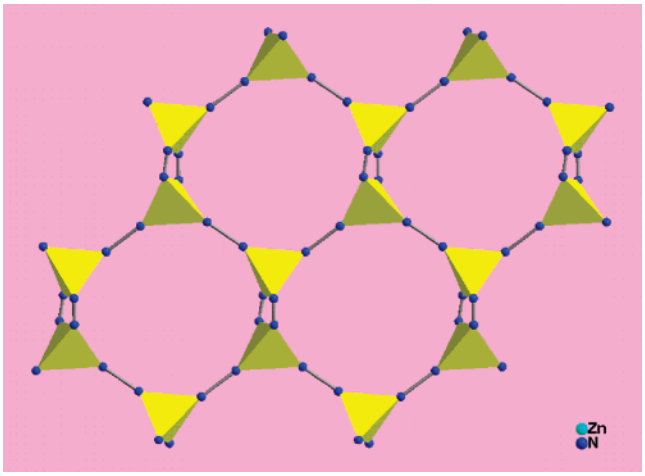

Figure 9. 2D framework of **3** highlighting the Zn tetrahedron. The line represents 5-(4-methylbenzo)tetrazole.

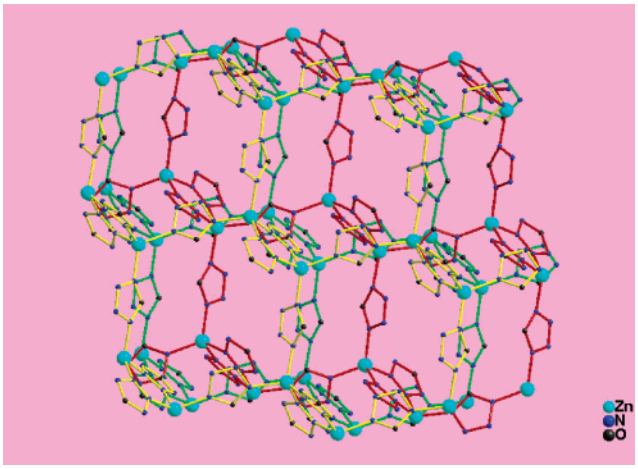

Figure 10. Packing arrangement (...ABAB...) representation of the adjacent layers in **3**. The tetrazole unit represents 5-(4-methylbenzo)tetrazole.

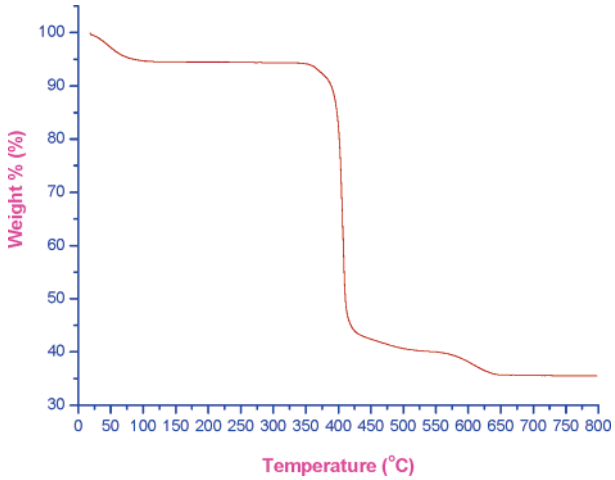

Figure 11. TGA view of compound **1**.

geometry around Zn centers may be more likely due to the direct reaction of Zn^{2+} with tetrazole preferring to give the thermodynamically more stable tetrahedron product. Nonetheless, the in situ formation of **1** and **2** supports the proposal that reaction between the inorganic azide and organic nitrile compound in the presence of a Lewis acid occurs via [2+3] cycloaddition mechanism.[5g]

Thermal Stabilities and Luminescent Properties of 1−3. In this work, we have examined the thermal stability of **1**. The open channels make it possible to remove the guest molecules from $[Zn(CH_3CN_4)_2]_3(H_2O)$ (**1**). Thermogravimetric analysis (TGA) of a polycrystalline sample of **1** revealed that one discrete weight loss (3.04%) occurred at 20∼80 °C, which is consistent with the removal of one water molecule per subunit (2.92% calculated). There is no weight loss for **1** until a temperature above 350 °C is reached, presumably due to decomposition of the network (Figure 11). The resulting solid, $[Zn(CH_3CN_4)_2]_3$, retains the framework and crystallinity, which is supported by consistent powder X-ray patterns for $[Zn(CH_3CN_4)_2]_3(H_2O)$ and $[Zn(CH_3CN_4)_2]_3$. The porous nature of $[Zn(CH_3CN_4)_2]_3$ was further demonstrated by its ability to absorb water vapor and regenerate **1**. The dehydration and rehydration processes were shown to be reversible.

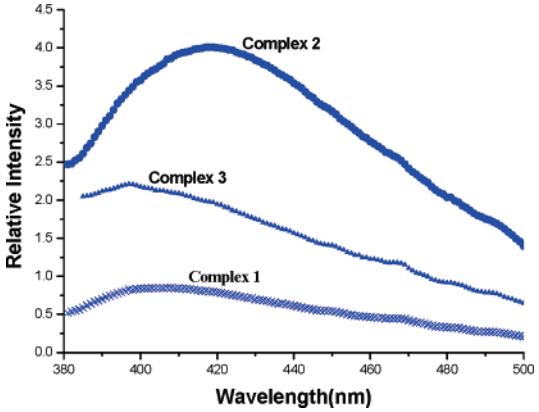

Figure 12. Fluorescent emission spectra of **1**, **2**, and **3** in the solid state at room temperature (λ_{ex} = 355 nm).

Aromatic organic molecules, all organic polymers, and mixed inorganic−organic hybrid coordination polymers have been investigated for fluorescence properties and for potential applications as fluorescence-emitted materials.[8] Owing to the ability of organic materials to affect wavelength emissions, syntheses of inorganic−organic coordination polymers by the judicious choice of organic spacers and metal centers (such as Zn, Cd, Pb, Ca, B, etc.) can be an efficient method to obtain new types of luminescent materials.[9] Of particular interest is the photoluminescent spectra of powdered **1**, **2**, and **3**. As shown in Figure 12, the solid-state fluorescent spectra of **1**, **2**, and **3** at room temperature reveal maximal emission peaks at 396, 418, and 397 nm, respectively. The results suggest that these complexes may be good blue-light-emitted materials. The photoluminescent mechanism is tentatively attributed to ligand-to-1igand transitions that are in reasonable agreement with literature examples on this class of zinc coordination polymers previously reported in our group and by others.[10]

Conclusions

In this article, we describe the synthesis of three novel zinc coordination polymers containing tetrazolyl ligands. By employing the in situ Demko−Sharpless [2+3] cycloaddition synthesis, reactions of acetonitrile or *p*-tolylnitrile with sodium azide in the presence of zinc perchlorate as a Lewis acid under hydrothermal (solvothermal) conditions gave **1** and **3** in good yields, respectively. The synthesis of **2** was obtained in good yield by directly reacting tetrazole with zinc acetate under hydrothermal reaction conditions. X-ray crystallographic analysis revealed that the structure of **1**

(8) Bunz, U. H. F. *Chem. Rev*. **2000**, *100*, 1605.
(9) (a) Ciurtin, D. M.; Pschirer, N. G.; Smith, M. D.; Bunz, U. H. F.; zur Loye, H.-C. *Chem. Mater*. **2001**, *13*, 2743. (b) Cariati, E.; Bu, X.; Ford, P. C. *Chem. Mater*. **2000**, *12*, 3385. (c) Würthner, F.; Sautter, A. *Chem. Commun*. **2000**, 445. (d) Dong, Y.-B.; Wang, P.; Huang, R.-Q.; Smith, M. D. *Inorg. Chem*. **2004**, *43*, 4727−4739.
(10) (a) Xiong, R.-G.; Zuo, J.-L.; You, X.-Z.; Abrahams, B. F.; Bai, Z.-P.; Che, C.-M.; Fun, H.-K. *Chem. Commun*. **2000**, 2061. (b) Xiong, R.-G.; Zuo, J.-L.; You, X.-Z.; Fun, H.-K.; Raj, S. S. S. *Organometallics* **2000**, *19*, 4183. (c) Fun, H.-K.; Raj, S. S. S.; Xiong, R.-G.; Zuo, J.-L.; Yu, Z.; You, X.-Z. *J. Chem. Soc., Dalton Trans*. **1999**, 1915. (d) Zhang, J.; Lin, W. B.; Chen, Z.-F.; Xiong, R.-G.; Abrahams, B. F.; Fun, H.-K.; *J. Chem. Soc., Dalton Trans*. **2001**, 1804. (e) Ye, Q.; Wang, X.-S.; Zhao, H.; Xiong, R.-G. *Chem. Soc. Rev*. **2005**, *34*, 208.

Table 2. Bond Lengths [Å] and Angles [deg] for **1**[a]

Zn(1)−N(2)#1	2.163(5)	Zn(1)−N(2)	2.163(5)
Zn(1)−N(2)#2	2.163(5)	Zn(1)−N(2)#3	2.163(5)
Zn(1)−N(2)#4	2.163(5)	Zn(1)−N(2)#5	2.163(5)
Zn(2)−N(1)#6	2.166(4)	Zn(2)−N(1)	2.166(4)
Zn(2)−N(1)#7	2.166(4)	Zn(2)−N(1)#8	2.166(4)
Zn(2)−N(1)#9	2.166(4)	Zn(2)−N(1)#1	2.166(4)
N(2)−N(1)#10	1.320(5)	N(2)−N(1)	1.320(5)
N(1)−C(3)	1.318(6)	C(3)−N(3)#10	1.345(11)
C(3)−C(3)#10	1.345(11)	C(3)−C(2)	1.458(14)
N(2)#1−Zn(1)−N(2)	90.0	N(2)#1−Zn(1)−N(2)#2	90.0
N(2)−Zn(1)−N(2)#2	180.0	N(2)#1−Zn(1)−N(2)#3	90.0
N(2)−Zn(1)−N(2)#3	90.0	N(2)#2−Zn(1)−N(2)#3	90.0
N(2)#1−Zn(1)−N(2)#4	90.0	N(2)−Zn(1)−N(2)#4	90.0
N(2)#2−Zn(1)−N(2)#4	90.0	N(2)#3−Zn(1)−N(2)#4	180.0
N(2)#1−Zn(1)−N(2)#5	180.0	N(2)−Zn(1)−N(2)#5	90.0
N(2)#2−Zn(1)−N(2)#5	90.0	N(2)#3−Zn(1)−N(2)#5	90.0
N(2)#4−Zn(1)−N(2)#5	90.0	N(1)#6−Zn(2)−N(1)	180.00(11)
N(1)#6−Zn(2)−N(1)#7	90.40(14)	N(1)−Zn(2)−N(1)#7	89.60(14)
N(1)#6−Zn(2)−N(1)#8	89.60(14)	N(1)−Zn(2)−N(1)#8	90.40(14)
N(1)#7−Zn(2)−N(1)#8	89.60(14)	N(1)#6−Zn(2)−N(1)#9	90.40(14)
N(1)−Zn(2)−N(1)#9	89.60(14)	N(1)#7−Zn(2)−N(1)#9	90.40(14)
N(1)#8−Zn(2)−N(1)#9	180.00(19)	N(1)#6−Zn(2)−N(1)#1	89.60(14)
N(1)−Zn(2)−N(1)#1	90.40(14)	N(1)#7−Zn(2)−N(1)#1	180.00(19)
N(1)#8−Zn(2)−N(1)#1	90.40(14)	N(1)#9−Zn(2)−N(1)#1	89.60(14)
N(1)#10−N(2)−N(1)	108.7(5)	N(1)#10−N(2)−Zn(1)	125.7(2)
N(1)−N(2)−Zn(1)	125.7(2)	C(3)−N(1)−N(2)	108.0(4)
C(3)−N(1)−Zn(2)	127.4(3)	N(2)−N(1)−Zn(2)	124.6(3)
N(1)#10−N(2)−N(1)	108.7(5)	C(3)−N(1)−N(2)	108.0(4)
N(1)−C(3)−N(3)#10	107.7(3)	N(1)−C(3)−C(3)#10	107.7(3)
N(3)#10−C(3)−C(3)#10	0.0(6)	N(1)−C(3)−C(2)	137.9(8)
N(3)#10−C(3)−C(2)	114.4(7)	C(3)#10−C(3)−C(2)	114.4(7)

[a] Symmetry transformations used to generate equivalent atoms: #1 $-y + 3/4$, $z + 0$, $-x + 3/4$; #2 $-x + 5/4$, $-y + 1/4$, $z + 0$; #3 $z + 1/2$, $x - 1/2$, y; #4 $z + 1/2$, $-x + 3/4$, $-y + 1/4$; #5 $y + 1/2$, z, $x - 1/2$; #6 $-x + 1$, $-y + 1/2$, $-z + 1/2$; #7 $y + 1/4$, $-z + 1/2$, $x - 1/4$; #8 $-z + 3/4$, $-x + 3/4$, $y + 0$; #9 $z + 1/4$, $x - 1/4$, $-y + 1/2$; #10 $x + 0$, $-y + 1/4$, $-z + 1/4$.

shows a super-diamond-like topological network with a diamond subunit as the connecting node. Although the structure of **2** also possesses a diamond-like topological network, it is 2-fold interpenetrated, and the structure of **3** was revealed to be a 2D layered network with a hexagonal net while the adjacent layers in the network stacked in an ABAB sequence. All three Zn complexes were demonstrated to display strong blue fluorescence emissions in the solid state at room temperature, which suggested that they may be good blue-light-emitted materials. The porous nature of **1** suggests it may have possible applications as a reversible zeolite analogue. Furthermore, the formation of **1** and **3** under the Demko−Sharpless tetrazole synthesis conditions affords us further insight on the nature of such reactions that includes what type of intermediates are formed during the reaction. The work described also provides strong encouragement for the construction of novel supramolecular arrays from the synthesis of metal coordination polymers by the hydrothermal generation of bridging ligands in the presence of appropriate metal ions.

Experimental Section

Caution! Metal azides may be explosive. Zinc−tetrazolate compounds may be shock-/metal-sensitive when ground with a metal spatula during preparation of KBr pellets for IR spectroscopic measurements. At all times, great care must be taken when handling these materials!

Materials and Methods. 5*H*-Tetrazole was prepared following literature methods.[2] 4-Methylbenzonitrile was purchased from Acros and used without further purification. All commercially available chemicals and solvents were of reagent grade and used as received. Fourier transform infrared (FTIR) spectra were measured as KBr

Table 3. Bond Lengths [Å] and Angles [deg] for **2**[a]

Zn(1)−N(8)	1.971(2)	Zn(1)−N(2)#1	1.976(2)
Zn(1)−N(3)#2	1.979(2)	Zn(1)−N(9)	1.987(2)
N(3)−Zn(1)#3	1.979(2)	N(2)−Zn(1)#4	1.976(2)
N(9)−C(1)	1.309(3)	N(9)−N(5)	1.338(3)
N(8)−C(2)	1.302(3)	N(8)−N(11)	1.346(3)
C(2)−N(2)	1.309(3)	C(1)−N(3)	1.305(3)
N(5)−N(4)	1.287(3)	N(4)−N(3)	1.344(3)
N(2)−N(1)	1.342(3)	N(1)−N(11)	1.291(3)
N(8)−Zn(1)−N(2)#1	111.07(9)	N(8)−Zn(1)−N(3)#2	112.74(9)
N(2)#1−Zn(1)−N(3)#2	108.65(10)	N(8)−Zn(1)−N(9)	106.89(9)
N(2)#1−Zn(1)−N(9)	110.05(10)	N(3)#2−Zn(1)−N(9)	107.37(9)
C(1)−N(9)−Zn(1)	134.1(2)	N(5)−N(9)−Zn(1)	120.34(19)
C(2)−N(8)−Zn(1)	131.78(19)	N(11)−N(8)−Zn(1)	122.56(18)
C(1)−N(3)−Zn(1)#3	132.0(2)	N(4)−N(3)−Zn(1)#3	121.95(19)
C(2)−N(2)−Zn(1)#4	132.2(2)	N(1)−N(2)−Zn(1)#4	122.28(18)
C(1)−N(9)−N(5)	105.3(2)	N(8)−C(2)−N(2)	111.4(3)
N(3)−C(1)−N(9)	111.3(3)	N(4)−N(5)−N(9)	109.1(2)
N(5)−N(4)−N(3)	108.8(2)	C(1)−N(3)−N(4)	105.4(2)
C(2)−N(2)−N(1)	105.4(2)	N(11)−N(1)−N(2)	109.0(2)
N(1)−N(11)−N(8)	108.6(2)		

[a] Symmetry transformations used to generate equivalent atoms: #1 $x + 1/2$, $-y + 1/2$, $-z + 1$; #2 $-x + 2$, $y - 1/2$, $-z + 1/2$; #3 $-x + 2$, $y + 1/2$, $-z + 1/2$; #4 $x - 1/2$, $-y + 1/2$, $-z + 1$.

Table 4. Bond Lengths [Å] and Angles [deg] for **3**[a]

Zn(1)−N(8)	1.963(5)	Zn(1)−N(8)#1	1.963(5)
Zn(1)−N(6)	1.993(5)	Zn(1)−N(6)#1	1.993(5)
N(8)−C(16)	1.337(6)	N(8)−N(3)	1.365(6)
N(7)−N(6)	1.311(6)	N(7)−N(4)	1.339(6)
N(7)−Zn(2)#2	1.970(6)	N(6)−N(5)	1.353(6)
C(16)−N(2)	1.332(6)	C(16)−C(14)	1.456(7)
N(5)−C(15)	1.331(8)	N(4)−C(15)	1.339(8)
C(15)−C(12)	1.459(8)	N(3)−N(1)	1.293(6)
C(14)−C(13)	1.384(7)	C(14)−C(9)	1.374(7)
C(13)−C(10)	1.374(7)	C(12)−C(4)	1.375(10)
C(12)−C(8)	1.363(10)	C(11)−C(5)	1.363(9)
C(11)−C(10)	1.390(8)	C(11)−C(2)	1.511(8)
C(9)−C(5)	1.366(8)	C(8)−C(7)	1.366(8)
C(7)−C(6)	1.343(13)	C(6)−C(1)	1.398(12)
C(6)−C(3)	1.516(9)	C(4)−C(1)	1.398(9)
N(2)−N(1)	1.350(6)	N(2)−Zn(2)	1.976(4)
Zn(2)−N(2)#3	1.976(4)	Zn(2)−N(7)#4	1.970(6)
Zn(2)−N(7)#5	1.970(6)		
N(8)−Zn(1)−N(8)#1	122.7(3)	N(8)−Zn(1)−N(6)	107.1(2)
N(8)#1−Zn(1)−N(6)	106.9(2)	N(8)−Zn(1)−N(6)#1	106.9(2)
N(8)#1−Zn(1)−N(6)#1	107.1(2)	N(6)−Zn(1)−N(6)#1	105.0(4)
C(16)−N(8)−N(3)	107.1(5)	C(16)−N(8)−Zn(1)	136.2(4)
N(3)−N(8)−Zn(1)	116.5(4)	N(6)−N(7)−N(4)	109.9(6)
N(6)−N(7)−Zn(2)#2	127.5(6)	N(4)−N(7)−Zn(2)#2	122.5(6)
N(7)−N(6)−N(5)	109.0(5)	N(7)−N(6)−Zn(1)	127.1(6)
N(5)−N(6)−Zn(1)	123.5(5)	N(8)−C(16)−N(2)	108.0(5)
N(8)−C(16)−C(14)	125.5(5)	N(2)−C(16)−C(14)	126.4(6)
C(15)−N(5)−N(6)	104.8(6)	N(7)−N(4)−C(15)	104.7(6)
N(5)−C(15)−C(12)	124.4(9)	N(4)−C(15)−C(12)	124.1(9)
N(1)−N(3)−N(8)	108.4(5)	C(13)−C(14)−C(9)	118.3(6)
C(13)−C(14)−C(16)	119.7(6)	C(9)−C(14)−C(16)	121.9(6)
C(10)−C(13)−C(14)	120.1(6)	C(4)−C(12)−C(8)	117.7(7)
C(4)−C(12)−C(15)	120.7(9)	C(8)−C(12)−C(15)	121.6(9)
C(5)−C(11)−C(10)	117.0(7)	C(5)−C(11)−C(2)	122.2(7)
C(10)−C(11)−C(2)	120.8(8)	C(13)−C(10)−C(11)	121.6(7)
C(5)−C(9)−C(14)	120.7(7)	C(12)−C(8)−C(7)	122.1(9)
C(6)−C(7)−C(8)	122.2(10)	C(7)−C(6)−C(1)	117.0(9)
C(7)−C(6)−C(3)	123.9(11)	C(1)−C(6)−C(3)	119.1(11)
C(9)−C(5)−C(11)	122.3(7)	C(12)−C(4)−C(1)	119.9(9)
C(4)−C(1)−C(6)	121.1(10)	C(16)−N(2)−N(1)	107.7(5)
N(1)−N(2)−Zn(2)	117.7(4)	N(3)−N(1)−N(2)	108.8(5)
N(2)−Zn(2)−N(2)#3	108.1(3)	N(2)−Zn(2)−N(7)#4	111.1(2)
N(2)#3−Zn(2)−N(7)#4	110.4(2)	N(2)−Zn(2)−N(7)#5	110.4(2)
N(2)#3−Zn(2)−N(7)#5	111.1(2)	N(7)#4−Zn(2)−N(7)#5	105.8(4)
N(5)−C(15)−N(4)	111.6(6)		

[a] Symmetry transformations used to generate equivalent atoms: #1 $-x$, y, $-z + 1/2$; #2 $x + 1/2$, $y + 1/2$, $-z + 1/2$; #3 $-x - 1$, y, $-z + 1/2$; #4 $x - 1/2$, $y - 1/2$, $-z + 1/2$; #5 $-x - 1/2$, y - 1/2, z.

pellets using a Nicolet FT-IR 17SX. TGA measurements were conducted on a TA-SDT 2960 with a heating rate of 5 °C/ min from 20 to 600 °C under a flux of nitrogen. Elemental analyses were performed on a Perkin−Elmer model 240C analyzer. Photoluminescent measurements were conducted on a Perkin−Elmer LS50B.

Preparation of $[Zn(CH_3CN_4)_2]_3(H_2O)$ (1). Hydrothermal treatment of $Zn(ClO_4)_2 \cdot 6H_2O$ (4 mmol), acetonitrile (6 mmol), NaN_3 (6 mmol), EtOH (5 mL), and water (12 mL) in an autoclave, sealed and placed in oven over 3 days at 125 °C, yielded a colorless prismatic crystalline product. The yield of **1** was about 60% based on the amount of acetonitrile consumed. Anal. Calcd for $C_{12}H_{20}N_{24}OZn_3$ (**1**): C, 20.21; H, 2.81; N, 47.15. Found: C, 21.15; H, 2.76; N, 48.32. IR (KBr, cm^{-1}): 3550 (br, s), 3475 (w), 2951 (w), 1611 (m), 1489 (s), 1381 (s), 1250 (m), 1182 (s), 1097 (w), 1041 (w), 700 (s), 603 (w), 445 (w).

Preparation of $C_2H_2N_8Zn$ (2). Hydrothermal treatment of $Zn(Ac)_2 \cdot 6H_2O$ (4 mmol), tetrazole (6 mmol), and 2-butanol (17 mL) in an autoclave, sealed and placed in oven over 3 days at 140 °C, yielded a colorless prismatic crystalline product. The yield of **2** was about 65% based on the amount of 5H-tetrazole consumed. Anal. Calcd for $C_2H_2N_8Zn$ (**3**): C, 6.88; H, 0.98; N, 55.04. Found: C, 6.60; H, 1.12; N, 56.03. IR (KBr, cm^{-1}): 3550 (br, s), 3444 (br, w), 3151 (s), 1474 (vs), 1367 (m), 1346 (m), 1259 (m), 1166 (s), 1104 (s), 1082 (s), 1006 (s), 998 (s), 891 (m), 884 (s), 680 (s).

Preparation of $C_{16}H_{14}N_8Zn$ (3). Hydrothermal treatment of $Zn(ClO_4)_2 \cdot 6H_2O$ (4 mmol), 4-methylbenzonitrile (6 mmol), NaN_3 (6 mmol), EtOH (5 mL), and water (12 mL) in an autoclave, sealed and placed in oven over 3 days at 125 °C, yielded a colorless prismatic crystalline product. The yield of **3** was about 75% based on the amount of 4-methylbenzonitrile consumed. Anal. Calcd for $C_{16}H_{14}N_8Zn$ (**3**): C, 50.04; H, 3.65; N, 29.19. Found: C, 49.97; H, 3.60; N, 30.15. IR (KBr, cm^{-1}): 3439 (br, w), 3026 (w), 2930 (w), 1616 (m), 1540 (w), 1470 (s), 1450 (s), 1388 (m), 1314 (w), 1289 (w), 1204 (m), 1156(w), 1121(m), 1074 (m), 1024 (w), 944 (w), 826 (s), 754 (s), 624 (w), 507 (m), 464 (m).

X-ray Structure Data. Crystallographic measurements were carried out using a Bruker SMART CCD diffractometer, ω scans, graphite-monochromated Mo Kα radiation ($\lambda = 0.71073$ Å), SAINT for data integration, SADABS for absorption correction, and XPREP for correction of Lorenz and polarization effects, and the structures were solved by direct methods and refined by full-matrix least-squares on $F2$ values using the SHELXS-97 (version 5.1) package of crystallographic software.[11] All non-hydrogen atoms (sometimes excluding those of solvent molecules) were refined anisotropically. Hydrogen atoms were generated and included in the structure factor calculations with assigned isotropic thermal parameters but were not refined. For the full-matrix least-squares refinements [$I > 2\sigma(I)$], the unweighted and weighted agreement factors of $R1 = \sum(F_o - F_c)/\sum F_o$ and $wR2 = [\sum w(F_o^2 - F_c^2)^2/\sum wF_o^4]^{1/2}$ were used. The crystal data and details of the structure determinations are summarized in Table 1. Selected bond distances and angles are listed in Table 2 (for **1**), Table 3 (for **2**), and Table 4 (for **3**).

Acknowledgment. This work was funded by The Major State Basic Research Development Program (Grant No. G2000077500) and the National Natural Science Foundation of China as well as the Distinguished Young Scholar Fund to R.-G.X. from the National Natural Science Foundation of China (2025103), EYTP of MOE (PRC), and BK2003204 (PRC). R.-G.X thanks the reviewers for their excellent and valuable suggestions and Prof. Z. Xue for the revision of this manuscript.

Supporting Information Available: X-ray data in CIF format and an additional figure. This material is available free of charge via the Internet at http://pubs.acs.org.

IC050354X

(11) *SMART*, version 5.624; *SAINT*, version 6.02; *SADABS*; *SHELXTL*, version 5.1; Bruker Analytical X-ray Systems, Inc.: Madison, WI, 1998.